SARS-CoV-2 is sensitive to type I interferon pretreatment.

Kumari G. Lokugamage[1], Adam Hage[1], Craig Schindewolf[1], Ricardo Rajsbaum[1,2], Vineet D. Menachery[1,2]

[1]Department of Microbiology and Immunology, [2]Institute for Human Infection and Immunity, University of Texas Medical Branch, Galveston TX, USA

Corresponding Author: Vineet D. Menachery

Address: University of Texas Medical Branch, 301 University Blvd, Route #0610 Galveston, TX 77555

Email: Vimenach@utmb.edu

Article Summary: SARS-CoV-2 has similar replication kinetics to SARS-CoV, but demonstrates significant sensitivity to type I interferon treatment.

Running title: SARS-CoV-2 sensitive to type I IFN pretreatment

Keywords: Coronavirus, 2019-nCoV, SARS-CoV-2, COVID-19, SARS-CoV, type I interferon, IFN

Abstract

SARS-CoV-2, a novel coronavirus (CoV), has recently emerged causing an ongoing outbreak of viral pneumonia around the world. While genetically distinct from the original SARS-CoV, both group 2B CoVs share similar genome organization and origins to coronaviruses harbored in bats. Importantly, initial guidance has used insights from SARS-CoV infection to inform treatment and public health strategies. In this report, we evaluate type-I Interferon (IFN-I) sensitivity of SARS-CoV-2 relative to the original SARS-CoV. Our results indicate that while SARS-CoV-2 maintains similar viral replication kinetics to SARS-CoV in Vero cell, the novel CoV is much more sensitive to IFN-I pretreatment. Examining transcriptional factor activation and interferon stimulated gene (ISG) induction, SARS-CoV-2 in the context of type I IFN induces phosphorylation of STAT1 and increased ISG proteins. In contrast, the original SARS-CoV has no evidence for STAT1 phosphorylation or ISG protein increases even in the presence of type I IFN pretreatment. Next, we examined IFN competent Calu3 2B4 cells finding SARS-CoV-2 had reduced viral replication relative to SARS-CoV and induced STAT1 phosphorylation late during infection. Finally, we examined homology between SARS-CoV and SARS-CoV-2 in viral proteins shown to be interferon antagonist. The absence of open reading frame (ORF) 3b and significant changes to ORF6 suggest the two key IFN antagonists may not maintain equivalent function in SARS-CoV-2. Together, the results identify key differences in susceptibility to the IFN-I response between SARS-CoV and SARS-CoV-2. that could help inform disease progression, treatment options, and animal model development.

Importance

With the ongoing outbreak of COVID-19 disease, differences between the SARS-CoV-2 and the original SARS-CoV could be leveraged to inform disease progression and eventual treatment options. In addition, these findings could have key implications for animal model development as well as further research into how SARS-CoV-2 modulates the type I IFN response early during infection.

Introduction

At the end of 2019, a cluster of patients in Hubei Province, China was diagnosed with a viral pneumonia of unknown origins. With community links to the Hunnan seafood market in Wuhan, the disease cluster had echoes of the severe acute respiratory syndrome coronavirus (SARS-CoV) outbreak that emerged at the beginning of the century (1). The 2019 etiologic agent was identified as a novel coronavirus, 2019-nCoV, and subsequently renamed SARS-CoV-2 (2). The new virus has nearly 80% nucleotide identity to the original SARS-CoV and the corresponding CoV disease, COVID-19, has many of the hallmarks of SARS-CoV disease including fever, breathing difficulty, bilateral lung infiltration, and death in the most extreme cases (3, 4). In addition, the most severe SARS-CoV-2 disease corresponded to old age (>50 years old), health status, and health care workers, similar to both SARS and MERS-CoV (5). Together, the results indicate SARS-CoV-2 infection and disease have strong similarity to the original SARS-CoV epidemic occurring nearly two decades earlier.

In the wake of the outbreak, major research efforts have sought to rapidly characterize the novel CoV to aid in treatment and control. Initial modeling studies predicted (6) and subsequent cell culture studies confirmed that spike protein of SARS-CoV-2 utilizes human angiotensin converting enzyme 2 (ACE2) for entry, the same receptor as SARS-CoV (7, 8). Extensive case studies indicated a similar range of disease onset and severe symptoms seen with SARS-CoV (5). Notably, less severe SARS-CoV-2 cases have also been observed and were not captured in the original SARS-CoV outbreak. Importantly, screening and treatment guidance has relied on previous CoV data generated with SARS-CoV and MERS-CoV. Treatments with both protease inhibitors and type I interferon (IFN-I) have been employed (4); similarly, remdesivir, a drug targeting viral polymerases, has been reported to have efficacy against SARS-CoV-2 similar to findings with both SARS- and MERS-CoV (9-12). Importantly, several vaccine efforts have been initiated with a focus on the SARS-CoV-2 spike protein as the

52 major antigenic determinate (13). Together, the similarities with SARS-CoV have been useful in
53 responding to the newest CoV outbreak.

54 The host Innate immune response is initiated when viral products are recognized by host
55 cell pattern recognition receptors, including Toll-like receptors (TLRs) and RIG-I-like receptors
56 (RLRs) (14, 15). This response ultimately results in production of IFN-I and other cytokines,
57 which together are essential for an effective antiviral response (16). IFN-I then triggers its own
58 signaling cascade via its receptor, in autocrine or paracrine manner, which induces
59 phosphorylation of signal transducers and activators of transcription 1 (STAT1) and STAT2.
60 Together, STAT1, STAT2, and a third transcription factor, IRF9, form the Interferon Stimulated
61 Gene Factor 3 (ISGF3) complex, which is essential for induction of many IFN-stimulated genes
62 (ISGs), and ultimately and effective antiviral response (17, 18). To establish productive
63 replication, viruses have developed different mechanisms to escape this antiviral response
64 targeting different parts of the IFN-I response machinery (19).

65 In this study, we further characterize SARS-CoV-2 and compare it to the original SARS-
66 CoV. Using Vero E6 cells, we demonstrate that SARS-CoV-2 maintains similar viral replication
67 kinetics as SARS-CoV following a low dose infection. In contrast, we find that SARS-CoV-2 is
68 much more sensitive to IFN-I pretreatment as compared to SARS-CoV. Examining further, we
69 determined that SARS-CoV-2 induces STAT1 phosphorylation and ISG expression, which is
70 absent in SARS-CoV. Similarly, infection of IFN competent Calu3 2B4 cells resulted in reduced
71 SARS-Cov-2 replication and STAT1 phosphorylation at late times. These results suggest
72 distinct changes between the CoVs in terms of IFN antagonism and we subsequently examined
73 sequence homology between the SARS-CoV and SARS-CoV-2 viral proteins that may be
74 responsible for these differences. Together, the results suggest SARS-CoV-2 lacks the same
75 capacity to control the IFN-I response as SARS-CoV.

76

77 **Results**

78 Our initial studies infected Vero E6 cells using a low multiplicity of infection (MOI) to
79 explore the viral replication kinetics of SARS-CoV-2 relative to SARS-CoV. Following infection,
80 we find that both SARS-CoV and SARS-CoV-2 replicate with similar kinetics, peaking 48 hours
81 post infection (**Fig. 1A**). While SARS-CoV-2 titer had slightly lower viral titers at 24 hours post
82 infection, the results were statistically different between the novel CoV and the original epidemic
83 strain. By 48 hours, replication of both viruses had plateaued and significant cytopathic effect
84 (CPE) was observed for both SARS-CoV and SARS-CoV-2 infections. Together, the results
85 indicated that SARS-CoV and SARS-CoV-2 replicate with similar replication kinetics in Vero E6
86 cells.

87 We next evaluated the susceptibility of SARS-CoV-2 to IFN-I pretreatment. Treatment
88 with IFN-I (recombinant IFNα) has been attempted as an antiviral approach for a wide variety of
89 pathogens including hepatitis B and C viruses as well as HIV (20). During both the SARS and
90 MERS-CoV outbreaks, IFN-I has been employed with limited effect (21, 22). In this study, we
91 pretreated Vero E6 cells with 1000 units of recombinant IFN-I (IFN-α) 18 hours prior to infection.
92 Vero E6 lack the capacity to produce IFN-I, but are able to respond to exogenous treatment
93 (23). Following pretreatment with IFN-I, SARS-CoV infection has a modest reduction in viral
94 titer (1.5 log plaque forming units (PFU) as compared to untreated control 24 hours post
95 infection (**Fig. 1B**). However, by 48 hours, SARS-CoV has nearly equivalent viral yields as the
96 untreated conditions (7.2 log PFU versus 7.5 log PFU). In contrast, SARS-CoV-2 shows a
97 significant reduction in viral replication following IFN-I treatment. At both 24 and 48 hours post
98 infection, SARS-CoV-2 had massive 3-log (24 HPI) and 4-log (48 HPI) drops in viral titer as
99 compared to control untreated cells. Finally, we examined viral protein production finding a
100 major deficit in nucleocapsid protein production in IFN-I treated cells following SARS-CoV-2
101 infection (**Fig. 1C**). In contrast, viral proteins were robustly expressed for SARS-CoV-2 in

102 untreated cells and for SARS-CoV in both conditions. Together, the results demonstrate a clear
103 sensitivity to a primed IFN-I response in SARS-CoV-2, which is not observed with SARS-CoV.

104 **SARS-CoV-2 fails to attenuate STAT1 phosphorylation and ISG production.**

105 To explore differences in IFN-I antagonism between SARS-CoV and SARS-CoV, we examined
106 both STAT1 activation and IFN stimulated gene (ISG) expression following IFN pretreatment
107 and infection. Examining Vero cell protein lysates, we found that IFN-I treated cells infected with
108 SARS-CoV-2 induced phosphorylated STAT-1 by 48 hours post infection (**Fig. 2**). STAT1
109 phosphorylation was absent in untreated cells infected with SARS-CoV-2 and suggest the novel
110 CoV is unable to inhibit a IFN-I preprimed response. In contrast, SARS-CoV had no evidence
111 for STAT1 phosphorylation in either IFN-I treated or untreated cells, illustrating robust control
112 over IFN-I induction pathways. Examining further, STAT1, IFIT2, and TRIM25, known ISGs (17),
113 had increased protein expression in the context of SARS-CoV-2 infection following IFN
114 pretreatment (**Fig. 2**). Basal STAT1 and TRIM25 levels are reduced during SARS-CoV and
115 SARS-CoV-2 infection relative to control likely due to the mRNA targeting activity of non-
116 structural protein 1 (NSP1) (24). However, IFN-I treatment results in augmented protein levels
117 for both ISGs following SARS-CoV-2 infection as compared to untreated control. In contrast,
118 IFN treated SARS-CoV had no significant increase in ISG protein relative to control infection.
119 Together, the STAT1 phosphorylation, ISG production, and viral protein levels indicate that
120 SARS-CoV-2 lacks the same capacity to modulate a primed type I IFN response as the original
121 SARS-CoV.

122 **SARS-CoV-2 induces STAT1 phosphorylation in interferon competent cells.**

123 While capable of responding to exogenous type I IFN, Vero cells lack the capacity to
124 produce type I IFN following infection which likely plays a role in robust replication of a wide
125 range of viruses []. To evaluate SARS-CoV-2 in a type I IFN responsive cell type, we infected

126 Calu3 2B4 cells, a lung epithelial cell line sorted for ACE2 expression and previously used in
127 coronavirus and influenza research (25). Using an MOI of 1, we examined the viral replication
128 kinetics of SARS-CoV-2 relative to SARS-CoV in Calu3 cells. We found that both SARS-CoV
129 and SARS-CoV-2 replicate with similar overall kinetics, peaking 24 hours post infection (**Fig.**
130 **3A**). However, SARS-CoV-2 replication is slightly attenuated relative to SARS-CoV at 24 hours
131 post infection (0.82 log reduction). The attenuation in viral replication expands at 48 hours (1.4
132 log reduction) indicating a significant change in total viral titers between SARS-CoV and SARS-
133 CoV-2. Notably, no similar attenuation was observed in untreated Vero cells (**Fig. 1A**)
134 suggesting possible immune modulation of SARS-CoV-2 infection.

135 To further evaluate type I IFN induction, we examined both STAT1 phosphorylation and
136 ISG expression following infection of Calu3 2B4 cells at 48 hours. Examining Calu3 cell protein
137 lysates, we found cells infected with SARS-CoV-2 induced phosphorylated STAT-1 by 48 hours
138 post infection (**Fig. 3B**). These results correspond to type I IFN treated Vero cell findings (**Fig.**
139 **2**) and suggest that the novel CoV is unable to completely inhibit the IFN-I response. In contrast,
140 SARS-CoV had no evidence for STAT1 phosphorylation Calu3 cells, illustrating robust control
141 over IFN-I induction pathways. Similar to the Vero IFN pretreatment, augmented levels of total
142 STAT1 was observed in SARS-CoV-2 relative SARS-CoV, although with not as dramatic an
143 increase. Similarly, TRIM25 was found to be reduced in both SARS-CoV and SARS-CoV-2
144 indicating that both viruses disrupt host protein production, likely due to mRNA antagonism by
145 CoV NSP1 (24). Overall, the data from Calu3 cells confirm that SARS-CoV-2 is unable to
146 maintain similar control over the IFN-I response as SARS-CoV.

147 **Conservation of IFN antagonists across SARS-CoV and SARS-CoV-2**

148 Considering the sensitivity to IFN-I, we next sought to evaluate changes between SARS-CoV
149 and SARS-CoV-2 viral proteins. Previous work has established several key IFN antagonist in
150 the SARS-CoV genome including NSP1, NSP3, ORF3b, ORF6, and others (26). Therefore, we

151 compared the sequence homology across viral proteins from SARS-CoV, SARS-CoV-2, and
152 several bat SARS-like viruses including WIV16-CoV (27), SHC014-CoV (28), and HKU3.1-CoV
153 (29). Using sequence analysis, we found several changes to SARS-CoV-2 that potentially
154 contribute to its type I IFN sensitivity (**Fig. 4**). For SARS-CoV structural proteins including the
155 nucleocapsid (N) and matrix (M) protein, a high degree of sequence homology (>90%AA
156 identity) suggests that their reported IFN antagonism is likely maintained in SARS-CoV-2 and
157 other SARS-like viruses. Similarly, the ORF1ab poly-protein retains high sequence identity in
158 SARS-CoV-2 and several known antagonists contained within the poly-protein (NSP1, NSP7,
159 NSP14-16) are highly conserved relative to SARS-CoV. One notable exception is the large
160 papain-like proteases, NSP3, which only 76% conserved between SARS-CoV and SARS-CoV-
161 2. However, SARS-CoV-2 does maintain a deubiquitinating domain thought to confer IFN
162 resistance (30). For SARS-CoV ORF3b, a 154 amino acid (AA) protein known to antagonize
163 the type I IFN responses by blocking IRF3 phosphorylation (31), sequence alignments indicates
164 that the SARS-CoV-2 equivalent ORF3b contains a premature stop codon resulting in a
165 truncated 24 AA protein. Similarly, HKU3.1-CoV also has a premature termination resulting in a
166 predicted 39 AA protein. Both WIV16-CoV and SHC014-CoV, the most closely related bat
167 viruses to SARS-CoV, encode longer 114 AA truncated protein with >99% homology with
168 SARS-CoV ORF3b suggesting that IFN antagonism might be maintained in these specific group
169 2B CoV strains. In addition, SARS-CoV ORF6 has been shown to be an IFN antagonist that
170 disrupts karyopherin transportation of transcriptions factors like STAT1 (31, 32). In contrast to
171 ORF3b, all five surveyed group 2B CoVs maintain ORF6; however, SARS-CoV-2 had only 69%
172 homology with SARS-CoV while the other three group 2B bat CoVs had >90% conservation.
173 Importantly, SARS-CoV-2 has a two amino acid truncation in its ORF6; previous work has found
174 that alanine substitution in this C-terminal of SARS-CoV ORF6 resulted in ablated antagonism
175 (32). Together, the sequence homology analysis suggests that differences in NSP3, ORF3b,
176 and/or ORF6 may be key drivers of SARS-CoV-2 type I IFN susceptibility.

177 **Discussion**

178 With the ongoing outbreak of COVID-19 caused by SARS-CoV-2, viral characterization remains
179 a key factor in responding to the emergent novel virus. In this report, we describe differences in
180 the IFN-I sensitivity between SARS-CoV-2 and the original SARS-CoV. While both viruses
181 maintain similar replication in untreated Vero E6 cells, SARS-CoV-2 has a significant decrease
182 in viral protein and replication following IFN-I pretreatment. The decreased SARS-CoV-2
183 replication correlates with phosphorylation of STAT1 and augmented ISG expression largely
184 absent following SARS-CoV infection despite IFN-I pretreatment. Notably, infection of IFN
185 competent Calu3 2B4 cells also resulted in reduced SARS-CoV-2 replication relative to SARS-
186 CoV. This modest reduction in viral replication corresponded to STAT1 phosphorylation in
187 SARS-CoV-2 infected Calu3 cells and indicated an inability to block type I IFN activation. the
188 sensitivity to IFN-I is distinct from the original SARS-CoV and suggests that the novel CoV has
189 distinct host interactions driving disease outcomes. Analysis of viral proteins finds SARS-CoV-2
190 has several changes that potentially impact its capacity to modulate the type I IFN response,
191 including loss of ORF3b and a short truncation of ORF6, both known as IFN-I antagonists for
192 SARS-CoV (31). Together, our results suggest SARS-CoV and SARS-CoV-2 have differences
193 in their ability to antagonize the IFN-I response once initiated and that they may have major
194 implication for COVID-19 disease and treatment.

195 With a similar genome organization and disease symptoms in humans, the SARS-CoV-2
196 outbreak has drawn insights from the closely related SARS-CoV. However, the differences in
197 sensitivity to IFN-I pretreatment illustrate a clear distinction between the two CoVs. Coupled with
198 a novel furin cleavage site (33), robust upper airway infection (8), and potential transmission
199 prior to symptomatic disease (34), the differences between SARS-CoV and SARS-CoV-2 could
200 prove important in disrupting the ongoing spread of COVID-19. For SARS-CoV, *in vitro* studies
201 have consistently found that wild-type SARS-CoV is indifferent to IFN-I pretreatment (35, 36).

202 Similarly, *in vivo* SARS-CoV studies have found that the loss of IFN-I signaling had no
203 significant impact on disease (37), suggesting that this virus is not sensitive to the antiviral
204 effects of IFN-I. However, more recent reports suggest that host genetic background may
205 majorly influence this finding (38). For SARS-CoV-2, our results suggest that IFN-I pretreatment
206 produces a 3 - 4 log drop in viral titer and correlates to STAT1 phosphorylation. This level of
207 sensitivity is similar to MERS-CoV and suggests that the novel CoV lacks the same capacity to
208 escape a primed IFN-I response as SARS-CoV (39, 40). Notably, the sensitivity to IFN-I does
209 not completely ablate viral replication; unlike SARS-CoV 2'O methyl-transferase mutants (35),
210 SARS-CoV-2 is able to replicate to low, detectable levels even in the presence of IFN-I. This
211 finding could help explain positive test in patients with minimal symptoms and the range of
212 disease observed. In addition, while SARS-CoV-2 is sensitive to IFN-I pretreatment, both
213 SARS-CoV and MERS-CoV employ effective means to disrupt virus recognition and
214 downstream signaling until late during infection (25). While SARS-CoV-2 may employ a similar
215 mechanism early during infection, STAT1 phosphorylation and reduced viral replication are
216 observed in IFN competent Calu3 indicating that the novel CoV does not as effectively block
217 IFN-I signaling as the original SARS-CoV

218 For SARS-CoV-2, the sensitivity to IFN-I indicates a distinction from SARS-CoV and
219 suggests differential host innate immune modulation between the viruses. The loss of ORF3b
220 and truncation/changes in ORF6 could signal a reduced capacity of SARS-CoV-2 to interfere
221 with type I IFN responses. For SARS-CoV ORF6, the N-terminal domain has been shown to
222 have a clear role in its ability to disrupt karyopherin transport (32); in turn, the loss of ORF6
223 function for SARS-CoV-2 would likely render it much more susceptible to IFN-I pretreatment as
224 activated STAT1 has the capacity to enter the nucleus and induce ISGs and the antiviral
225 response. In these studies, we have found that following IFN-I pretreatment, STAT1
226 phosphorylation is induced following SARS-CoV-2 infection. The increase in ISG proteins

227 (STAT1, IFIT2, TRIM25) suggests that SARS-CoV-2 ORF6 does not effectively block nuclear
228 transport as well as SARS ORF6. For SARS-CoV ORF3b, the viral protein has been shown to
229 disrupt phosphorylation of IRF3, a key transcriptional factor in the induction of IFN-I and the
230 antiviral state (31). While its mechanism of action is not clear, the ORF3b absence in SARS-
231 CoV-2 infection likely impacts its ability to inhibit the IFN-I response and eventual STAT1
232 activation. Similarly, while NSP3 deubiquitinating domain remains intact, SARS-CoV-2 has a 24
233 AA insertion upstream of this deubiquitinating domain that could potentially alter that function
234 (30). While other antagonists are maintained with high levels of conservation (>90%), single
235 point mutations in key locations could modify function and contribute to increased IFN
236 sensitivity. Overall, the sequence analysis suggests that differences between SARS-CoV and
237 SARS-CoV-2 viral proteins may drive attenuation in the context of type I IFN pretreatment.

238 The increased sensitivity of SARS-CoV-2 suggests utility in treatment using type I IFN.
239 While IFN-I has been used in response to chronic viral infection (41), previous examination of
240 SARS-CoV cases found inconclusive effect for type I IFN treatment (42). However, the findings
241 from the SARS-CoV outbreak were complicated by combination therapy of type I IFN with other
242 treatments including ribavirin/steroids and lack of a regimented protocol. While type I IFN has
243 been utilized to treat MERS-CoV infected patients, no conclusive data yet exists to determine
244 efficacy (43). Yet, *in vivo* studies with MERS-CoV has found that early induction with type I IFN
245 can be protective in mice (44); importantly, the same study found that late type I IFN induction
246 can be detrimental for MERS-CoV disease (44). Similarly, early reports have described
247 treatments using type I IFN in combination for SARS-CoV-2 infection; yet the efficacy of these
248 treatments and the parameters of their use are not known (45). Overall, sensitivity data suggest
249 that type I IFN treatment may have utility for treating SARS-CoV-2 if the appropriate parameters
250 can be determined. In addition, use of type III IFN, which is predicted to have utility in the
251 respiratory tract, could offer another means for effective treatment for SARS-CoV-2.

252 In addition to treatment, the sensitivity to type I IFN may also have implications for
253 animal model development. For SARS-CoV, mouse models that recapitulate human disease
254 were developed through virus passage in immune competent mice (46). Similarly, mouse
255 models for MERS-CoV required adaptation in mice that had genetic modifications of their
256 dipeptidyl-peptidase 4 (DPP4), the receptor for MERS-CoV (47, 48). However, each of these
257 MERS-CoV mouse models still retained full immune capacity. In contrast, SARS-CoV-2
258 sensitivity to type I IFN may signal the need to use an immune deficient model to develop
259 relevant disease. While initial work has suggested incompatibility to SARS-CoV-2 infection in
260 mice based on receptor usage (8), the type I IFN response may be a second major barrier that
261 needs to be overcome. Similar to the emergent Zika virus outbreak, the use of type I IFN
262 receptor knockout mice or type I IFN receptor blocking antibody may be necessary to develop a
263 useful SARS-CoV-2 animal models for therapeutic testing (49).

264 Overall, our results indicate that SARS-CoV-2 has a much higher sensitivity to type I IFN
265 than the previously emergent SARS-CoV. This augmented type I IFN sensitivity is likely due to
266 changes in viral proteins between the two epidemic CoV strains. Moving forward, these data
267 could provide important insights for both the treatment of SARS-CoV-2 as well as developing
268 novel animal models of disease. In this ongoing outbreak, the results also highlight a distinction
269 between the highly related viruses and suggest insights from SARS-CoV must be verified for
270 SARS-CoV-2 infection and disease.

271

272 **Methods**

273 **Viruses and cells.** SARS-CoV-2 USA-WA1/2020, provided by the World Reference Center for
274 Emerging Viruses and Arboviruses (WRCEVA) and was originally obtained from the USA
275 Centers of Disease Control as described(50). SARS-CoV-2 and mouse-adapted recombinant
276 SARS-CoV (MA15) (46) were titrated and propagated on VeroE6 cells, grown in DMEM with 5%
277 fetal bovine serum and 1% antibiotic/antimytotic (Gibco). Calu3 2B4 cells were grown in DMEM
278 with 10% defined fetal bovine serum, 1% sodium pyruvate (Gibco), and 1% antibiotic/antimitotic
279 (Gibco). Standard plaque assays were used for SARS-CoV and SARS-CoV-2 (51, 52). All
280 experiments involving infectious virus were conducted at the University of Texas Medical
281 Branch (Galveston, TX) in approved biosafety level 3 (BSL) laboratories with routine medical
282 monitoring of staff.

283 **Infection and type I IFN pretreatment.** Viral replication in Vero E6 and Calu3 2B4 cells were
284 performed as previously described (35, 53). Briefly, cells were washed with two times with PBS
285 and inoculated with SARS-CoV or SARS-CoV-2 at an multiplicity of infection (MOI) 0.01 for 60
286 minutes at 37 °C. Following inoculation, cells were washed 3 times, and fresh media was added
287 to signify time 0. Three or more biological replicates were harvested at each described time. No
288 blinding was used in any sample collections, nor were samples randomized. For type I IFN
289 pretreatment, experiments were completed as previously described (35). Briefly, Vero E6 cells
290 were incubated with 1000 units/mL of recombinant type I IFN alpha (PBL Assay Sciences) 18
291 hours prior to infection (35). Cells were infected as described above and type I IFN was not
292 added back after infection.

293 **Phylogenetic Tree and Sequence Identity Heat Map**. Heat maps were constructed from a set
294 of representative group 2B coronaviruses by using alignment data paired with neighbor-joining
295 phylogenetic trees built in Geneious (v.9.1.5). Sequence identity was visualized using EvolView
296 (http://evolgenius.info/) and utilized SARS-CoV Urbani as the reference sequence. Tree shows

297 the degree of genetic similarity of SARS-CoV-2 and SARS-CoV across a selected group 2B
298 coronaviruses

299 **Immunoblot Analysis and Antibodies:**

300 Viral and host protein analysis were evaluated as previously described (50, 54). Briefly, cell
301 lysates were resolved on 7.5% Mini-PROTEAN TGX SDS-PAGE gels and then transferred to
302 polyvinylidene difluoride (PVDF) membranes using a Trans-Blot Turbo transfer system (Bio-
303 Rad). Membranes were blocked with 5% (w/v) non-fat dry milk in TBST (TBS with 0.1% (v/v)
304 Tween-20) for 1 hr, and then probed with the indicated primary antibody in 3% (w/v) BSA in
305 TBST at 4°C overnight. Following overnight incubation, membranes were probed with the
306 following secondary antibodies in 5% (w/v) non-fat dry milk in TBST for 1 hr at room
307 temperature: anti-rabbit or anti-mouse IgG-HRP conjugated antibody from sheep (both 1:10,000
308 GE Healthcare). Proteins were visualized using ECL or SuperSignal West Femto
309 chemiluminescence reagents (Pierce) and detected by autoradiography. The following primary
310 antibodies were used: anti-pSTAT1 (Y701) (1:1000 9171L Cell Signaling Technologies), anti-
311 STAT1 D1K9Y (1:1000 14994P Cell Signaling Technologies), anti-IFIT2 (1:2000 PA3-845
312 Invitrogen), anti-TRIM25 (1:1000 610570 BD Biosciences), anti-SARS-CoV Nucleocapsid
313 (1:1000), and anti-β-Actin (1:1000 ab8227 Abcam).

314 **Statistical analysis.** All statistical comparisons in this manuscript involved the comparison
315 between 2 groups, SARS-CoV or SARS-CoV-2 infected groups under equivalent conditions.
316 Thus, significant differences in viral titer were determined by the unpaired two-tailed students T-
317 Test.

318 **Acknowledgements.** Research was supported by grants from NIA and NIAID of the NIH
319 (U19AI100625 and R00AG049092 to VDM; R24AI120942 to WRCEVA; R01AI134907 to RR;
320 and T32 AI060549 to AH). Research was also supported by STARs Award provided by the
321 University of Texas System to VDM and trainee funding provided by the McLaughlin Fellowship
322 Fund at UTMB.

References

1. **Gralinski LE, Menachery VD.** 2020. Return of the Coronavirus: 2019-nCoV. Viruses **12**.
2. **Gorbalenya AE, Baker SC, Baric RS, de Groot RJ, Drosten C, Gulyaeva AA, Haagmans BL, Lauber C, Leontovich AM, Neuman BW, Penzar D, Perlman S, Poon LLM, Samborskiy DV, Sidorov IA, Sola I, Ziebuhr J, Coronaviridae Study Group of the International Committee on Taxonomy of V.** 2020. The species Severe acute respiratory syndrome-related coronavirus: classifying 2019-nCoV and naming it SARS-CoV-2. Nature Microbiology doi:10.1038/s41564-020-0695-z.
3. **Zhu N, Zhang D, Wang W, Li X, Yang B, Song J, Zhao X, Huang B, Shi W, Lu R, Niu P, Zhan F, Ma X, Wang D, Xu W, Wu G, Gao GF, Tan W, China Novel Coronavirus I, Research T.** 2020. A Novel Coronavirus from Patients with Pneumonia in China, 2019. N Engl J Med **382:**727-733.
4. **Huang C, Wang Y, Li X, Ren L, Zhao J, Hu Y, Zhang L, Fan G, Xu J, Gu X, Cheng Z, Yu T, Xia J, Wei Y, Wu W, Xie X, Yin W, Li H, Liu M, Xiao Y, Gao H, Guo L, Xie J, Wang G, Jiang R, Gao Z, Jin Q, Wang J, Cao B.** 2020. Clinical features of patients infected with 2019 novel coronavirus in Wuhan, China. Lancet **395:**497-506.
5. **Wu Z, McGoogan JM.** 2020. Characteristics of and Important Lessons From the Coronavirus Disease 2019 (COVID-19) Outbreak in China: Summary of a Report of 72314 Cases From the Chinese Center for Disease Control and Prevention. JAMA doi:10.1001/jama.2020.2648.
6. **Xu X, Chen P, Wang J, Feng J, Zhou H, Li X, Zhong W, Hao P.** 2020. Evolution of the novel coronavirus from the ongoing Wuhan outbreak and modeling of its spike protein for risk of human transmission. Sci China Life Sci **63:**457-460.
7. **Letko M, Marzi A, Munster V.** 2020. Functional assessment of cell entry and receptor usage for SARS-CoV-2 and other lineage B betacoronaviruses. Nat Microbiol doi:10.1038/s41564-020-0688-y.
8. **Zhou P, Yang XL, Wang XG, Hu B, Zhang L, Zhang W, Si HR, Zhu Y, Li B, Huang CL, Chen HD, Chen J, Luo Y, Guo H, Jiang RD, Liu MQ, Chen Y, Shen XR, Wang X, Zheng XS, Zhao K, Chen QJ, Deng F, Liu LL, Yan B, Zhan FX, Wang YY, Xiao GF, Shi ZL.** 2020. A pneumonia outbreak associated with a new coronavirus of probable bat origin. Nature doi:10.1038/s41586-020-2012-7.
9. **de Wit E, Feldmann F, Cronin J, Jordan R, Okumura A, Thomas T, Scott D, Cihlar T, Feldmann H.** 2020. Prophylactic and therapeutic remdesivir (GS-5734) treatment in the rhesus macaque model of MERS-CoV infection. Proc Natl Acad Sci U S A doi:10.1073/pnas.1922083117.
10. **Wang M, Cao R, Zhang L, Yang X, Liu J, Xu M, Shi Z, Hu Z, Zhong W, Xiao G.** 2020. Remdesivir and chloroquine effectively inhibit the recently emerged novel coronavirus (2019-nCoV) in vitro. Cell Res doi:10.1038/s41422-020-0282-0.
11. **Sheahan TP, Sims AC, Leist SR, Schafer A, Won J, Brown AJ, Montgomery SA, Hogg A, Babusis D, Clarke MO, Spahn JE, Bauer L, Sellers S, Porter D, Feng JY, Cihlar T, Jordan R, Denison MR, Baric RS.** 2020. Comparative therapeutic efficacy of remdesivir and combination lopinavir, ritonavir, and interferon beta against MERS-CoV. Nat Commun **11:**222.
12. **Sheahan TP, Sims AC, Graham RL, Menachery VD, Gralinski LE, Case JB, Leist SR, Pyrc K, Feng JY, Trantcheva I, Bannister R, Park Y, Babusis D, Clarke MO, Mackman RL, Spahn JE, Palmiotti CA, Siegel D, Ray AS, Cihlar T, Jordan R, Denison MR, Baric RS.** 2017. Broad-spectrum antiviral GS-5734 inhibits both epidemic and zoonotic coronaviruses. Sci Transl Med **9**.
13. **Ahmed SF, Quadeer AA, McKay MR.** 2020. Preliminary Identification of Potential Vaccine Targets for the COVID-19 Coronavirus (SARS-CoV-2) Based on SARS-CoV Immunological Studies. Viruses **12**.

373 14. **Medzhitov R, Janeway CA, Jr.** 1997. Innate immunity: the virtues of a nonclonal
374 system of recognition. Cell **91:**295-298.
375 15. **Meylan E, Tschopp J.** 2006. Toll-like receptors and RNA helicases: two parallel ways to
376 trigger antiviral responses. Mol Cell **22:**561-569.
377 16. **Akira S.** 2006. TLR signaling. Curr Top Microbiol Immunol **311:**1-16.
378 17. **Schoggins JW, Wilson SJ, Panis M, Murphy MY, Jones CT, Bieniasz P, Rice CM.**
379 2011. A diverse range of gene products are effectors of the type I interferon antiviral response.
380 Nature **472:**481-485.
381 18. **Platanias LC.** 2005. Mechanisms of type-I- and type-II-interferon-mediated signalling.
382 Nat Rev Immunol **5:**375-386.
383 19. **Rajsbaum R, Garcia-Sastre A.** 2013. Viral evasion mechanisms of early antiviral
384 responses involving regulation of ubiquitin pathways. Trends Microbiol **21:**421-429.
385 20. **Lin FC, Young HA.** 2014. Interferons: Success in anti-viral immunotherapy. Cytokine
386 Growth Factor Rev **25:**369-376.
387 21. **Zumla A, Hui DS, Perlman S.** 2015. Middle East respiratory syndrome. Lancet
388 **386:**995-1007.
389 22. **Song Z, Xu Y, Bao L, Zhang L, Yu P, Qu Y, Zhu H, Zhao W, Han Y, Qin C.** 2019.
390 From SARS to MERS, Thrusting Coronaviruses into the Spotlight. Viruses **11**.
391 23. **Diaz MO, Ziemin S, Le Beau MM, Pitha P, Smith SD, Chilcote RR, Rowley JD.** 1988.
392 Homozygous deletion of the alpha- and beta 1-interferon genes in human leukemia and derived
393 cell lines. Proc Natl Acad Sci U S A **85:**5259-5263.
394 24. **Narayanan K, Ramirez SI, Lokugamage KG, Makino S.** 2015. Coronavirus
395 nonstructural protein 1: Common and distinct functions in the regulation of host and viral gene
396 expression. Virus Res **202:**89-100.
397 25. **Menachery VD, Eisfeld AJ, Schafer A, Josset L, Sims AC, Proll S, Fan S, Li C,**
398 **Neumann G, Tilton SC, Chang J, Gralinski LE, Long C, Green R, Williams CM, Weiss J,**
399 **Matzke MM, Webb-Robertson BJ, Schepmoes AA, Shukla AK, Metz TO, Smith RD, Waters**
400 **KM, Katze MG, Kawaoka Y, Baric RS.** 2014. Pathogenic influenza viruses and coronaviruses
401 utilize similar and contrasting approaches to control interferon-stimulated gene responses. mBio
402 **5:**e01174-01114.
403 26. **Totura AL, Baric RS.** 2012. SARS coronavirus pathogenesis: host innate immune
404 responses and viral antagonism of interferon. Curr Opin Virol **2:**264-275.
405 27. **Yang XL, Hu B, Wang B, Wang MN, Zhang Q, Zhang W, Wu LJ, Ge XY, Zhang YZ,**
406 **Daszak P, Wang LF, Shi ZL.** 2015. Isolation and Characterization of a Novel Bat Coronavirus
407 Closely Related to the Direct Progenitor of Severe Acute Respiratory Syndrome Coronavirus. J
408 Virol **90:**3253-3256.
409 28. **Ge XY, Li JL, Yang XL, Chmura AA, Zhu G, Epstein JH, Mazet JK, Hu B, Zhang W,**
410 **Peng C, Zhang YJ, Luo CM, Tan B, Wang N, Zhu Y, Crameri G, Zhang SY, Wang LF,**
411 **Daszak P, Shi ZL.** 2013. Isolation and characterization of a bat SARS-like coronavirus that
412 uses the ACE2 receptor. Nature **503:**535-538.
413 29. **Lau SK, Woo PC, Li KS, Huang Y, Tsoi HW, Wong BH, Wong SS, Leung SY, Chan**
414 **KH, Yuen KY.** 2005. Severe acute respiratory syndrome coronavirus-like virus in Chinese
415 horseshoe bats. Proc Natl Acad Sci U S A **102:**14040-14045.
416 30. **Clementz MA, Chen Z, Banach BS, Wang Y, Sun L, Ratia K, Baez-Santos YM, Wang**
417 **J, Takayama J, Ghosh AK, Li K, Mesecar AD, Baker SC.** 2010. Deubiquitinating and
418 interferon antagonism activities of coronavirus papain-like proteases. J Virol **84:**4619-4629.
419 31. **Kopecky-Bromberg SA, Martinez-Sobrido L, Frieman M, Baric RA, Palese P.** 2007.
420 Severe acute respiratory syndrome coronavirus open reading frame (ORF) 3b, ORF 6, and
421 nucleocapsid proteins function as interferon antagonists. J Virol **81:**548-557.
422 32. **Frieman M, Yount B, Heise M, Kopecky-Bromberg SA, Palese P, Baric RS.** 2007.
423 Severe acute respiratory syndrome coronavirus ORF6 antagonizes STAT1 function by

424 sequestering nuclear import factors on the rough endoplasmic reticulum/Golgi membrane. J
425 Virol **81:**9812-9824.
426 33. **Coutard B, Valle C, de Lamballerie X, Canard B, Seidah NG, Decroly E.** 2020. The
427 spike glycoprotein of the new coronavirus 2019-nCoV contains a furin-like cleavage site absent
428 in CoV of the same clade. Antiviral Res **176:**104742.
429 34. **Tong ZD, Tang A, Li KF, Li P, Wang HL, Yi JP, Zhang YL, Yan JB.** 2020. Potential
430 Presymptomatic Transmission of SARS-CoV-2, Zhejiang Province, China, 2020. Emerg Infect
431 Dis **26**.
432 35. **Menachery VD, Yount BL, Jr., Josset L, Gralinski LE, Scobey T, Agnihothram S,**
433 **Katze MG, Baric RS.** 2014. Attenuation and restoration of severe acute respiratory syndrome
434 coronavirus mutant lacking 2'-o-methyltransferase activity. J Virol **88:**4251-4264.
435 36. **Thiel V, Weber F.** 2008. Interferon and cytokine responses to SARS-coronavirus
436 infection. Cytokine Growth Factor Rev **19:**121-132.
437 37. **Frieman MB, Chen J, Morrison TE, Whitmore A, Funkhouser W, Ward JM,**
438 **Lamirande EW, Roberts A, Heise M, Subbarao K, Baric RS.** 2010. SARS-CoV pathogenesis
439 is regulated by a STAT1 dependent but a type I, II and III interferon receptor independent
440 mechanism. PLoS Pathog **6:**e1000849.
441 38. **Channappanavar R, Fehr AR, Vijay R, Mack M, Zhao J, Meyerholz DK, Perlman S.**
442 2016. Dysregulated Type I Interferon and Inflammatory Monocyte-Macrophage Responses
443 Cause Lethal Pneumonia in SARS-CoV-Infected Mice. Cell Host Microbe **19:**181-193.
444 39. **Menachery VD, Gralinski LE, Mitchell HD, Dinnon KH, 3rd, Leist SR, Yount BL, Jr.,**
445 **Graham RL, McAnarney ET, Stratton KG, Cockrell AS, Debbink K, Sims AC, Waters KM,**
446 **Baric RS.** 2017. Middle East Respiratory Syndrome Coronavirus Nonstructural Protein 16 Is
447 Necessary for Interferon Resistance and Viral Pathogenesis. mSphere **2**.
448 40. **Falzarano D, de Wit E, Martellaro C, Callison J, Munster VJ, Feldmann H.** 2013.
449 Inhibition of novel beta coronavirus replication by a combination of interferon-alpha2b and
450 ribavirin. Sci Rep **3:**1686.
451 41. **Finter NB, Chapman S, Dowd P, Johnston JM, Manna V, Sarantis N, Sheron N,**
452 **Scott G, Phua S, Tatum PB.** 1991. The use of interferon-alpha in virus infections. Drugs
453 **42:**749-765.
454 42. **Stockman LJ, Bellamy R, Garner P.** 2006. SARS: systematic review of treatment
455 effects. PLoS Med **3:**e343.
456 43. **de Wit E, van Doremalen N, Falzarano D, Munster VJ.** 2016. SARS and MERS:
457 recent insights into emerging coronaviruses. Nat Rev Microbiol **14:**523-534.
458 44. **Channappanavar R, Fehr AR, Zheng J, Wohlford-Lenane C, Abrahante JE, Mack M,**
459 **Sompallae R, McCray PB, Jr., Meyerholz DK, Perlman S.** 2019. IFN-I response timing
460 relative to virus replication determines MERS coronavirus infection outcomes. J Clin Invest
461 **130:**3625-3639.
462 45. **Pang J, Wang MX, Ang IYH, Tan SHX, Lewis RF, Chen JI, Gutierrez RA, Gwee**
463 **SXW, Chua PEY, Yang Q, Ng XY, Yap RK, Tan HY, Teo YY, Tan CC, Cook AR, Yap JC, Hsu**
464 **LY.** 2020. Potential Rapid Diagnostics, Vaccine and Therapeutics for 2019 Novel Coronavirus
465 (2019-nCoV): A Systematic Review. J Clin Med **9**.
466 46. **Roberts A, Deming D, Paddock CD, Cheng A, Yount B, Vogel L, Herman BD,**
467 **Sheahan T, Heise M, Genrich GL, Zaki SR, Baric R, Subbarao K.** 2007. A mouse-adapted
468 SARS-coronavirus causes disease and mortality in BALB/c mice. PLoS Pathog **3:**e5.
469 47. **Cockrell A YB, Scobey T, Jensen K, Douglas M, Beall A, Tang X-C, Marasco WA,**
470 **Heise MT, Baric RS** 2016. A Mouse Model for MERS Coronavirus Induced Acute Respiratory
471 Distress Syndrome. . Nature Microbiology **In Press**.
472 48. **Li K, Wohlford-Lenane CL, Channappanavar R, Park JE, Earnest JT, Bair TB, Bates**
473 **AM, Brogden KA, Flaherty HA, Gallagher T, Meyerholz DK, Perlman S, McCray PB, Jr.**

474 2017. Mouse-adapted MERS coronavirus causes lethal lung disease in human DPP4 knockin
475 mice. Proc Natl Acad Sci U S A **114:**E3119-E3128.
476 49. **Lazear HM, Govero J, Smith AM, Platt DJ, Fernandez E, Miner JJ, Diamond MS.**
477 2016. A Mouse Model of Zika Virus Pathogenesis. Cell Host Microbe **19:**720-730.
478 50. **Harcourt J, Tamin A, Lu X, Kamili S, Sakthivel SK, Murray J, Queen K, Tao Y,**
479 **Paden CR, Zhang J, Li Y, Uehara A, Wang H, Goldsmith C, Bullock HA, Wang L, Whitaker**
480 **B, Lynch B, Gautam R, Schindewolf C, Lokugamage KG, Scharton D, Plante JA,**
481 **Mirchandani D, Widen SG, Narayanan K, Makino S, Ksiazek TG, Plante KS, Weaver SC,**
482 **Lindstrom S, Tong S, Menachery VD, Thornburg NJ.** 2020. Severe Acute Respiratory
483 Syndrome Coronavirus 2 from Patient with 2019 Novel Coronavirus Disease, United States.
484 Emerg Infect Dis **26**.
485 51. **Sims AC, Tilton SC, Menachery VD, Gralinski LE, Schäfer A, Matzke MM, Webb-**
486 **Robertson BJ, Chang J, Luna ML, Long CE, Shukla AK, Bankhead AR, Burkett SE,**
487 **Zornetzer G, Tseng CT, Metz TO, Pickles R, McWeeney S, Smith RD, Katze MG, Waters**
488 **KM, Baric RS.** 2013. Release of severe acute respiratory syndrome coronavirus nuclear import
489 block enhances host transcription in human lung cells. J Virol **87:**3885-3902.
490 52. **Josset L, Menachery VD, Gralinski LE, Agnihothram S, Sova P, Carter VS, Yount**
491 **BL, Graham RL, Baric RS, Katze MG.** 2013. Cell host response to infection with novel human
492 coronavirus EMC predicts potential antivirals and important differences with SARS coronavirus.
493 MBio **4:**e00165-00113.
494 53. **Sheahan T, Rockx B, Donaldson E, Corti D, Baric R.** 2008. Pathways of cross-
495 species transmission of synthetically reconstructed zoonotic severe acute respiratory syndrome
496 coronavirus. J Virol **82:**8721-8732.
497 54. **van Tol S, Atkins C, Bharaj P, Johnson KN, Hage A, Freiberg AN, Rajsbaum R.**
498 2020. VAMP8 Contributes to the TRIM6-Mediated Type I Interferon Antiviral Response during
499 West Nile Virus Infection. J Virol **94**.

500

501

502 **Figure Legends**

503 **Figure 1. SARS-CoV-2 sensitive to type I IFN pretreatment.** A) Vero E6 cells infected with
504 either SARS-CoV WT (black) or SARS-CoV-2 (blue) at an MOI of 0.01. Media harvested at 4,
505 24, and 48 hours post infection. B) Vero E6 cells were treated with 1000 units recombinant type
506 I IFN or mock for 18 hours prior to infection. Cells were subsequently infected at with either
507 SARS-CoV WT (black) or SARS-CoV-2 (blue) at an MOI of 0.01 as described above. Each
508 point on the line graph represents the group mean, N=6 for 24 and 48HPI, N=3 for 3HPI. All
509 error bars represent SD. The two tailed students t-test was used to determine P-values: *** P <
510 0.001. C) Cell protein lysates from IFN treated and untreated cells were probed 48 hours post
511 infection by using Western blotting with rabbit polyclonal anti-SARS N antibody or actin.

512

513 **Figure 2. SARS-CoV-2 infection induces STAT1 phosphorylation and ISG production.**
514 Vero cell protein lysates from IFN-I treated and untreated cells were probed 48 hours post
515 infection by Western blotting for phosphorylated STAT1 (Y701), STAT1, IFIT2, TRIM25, and
516 Actin.

517

518 **Figure 3. SARS-CoV-2 induces STAT1 phosphorylation in IFN competent cells.** A) Calu
519 2B4 cells were infected with either SARS-CoV WT (black) or SARS-CoV-2 (blue) at an MOI of
520 1. Media harvested at 4, 24, and 48 hours post infection. Each point on the line graph
521 represents the group mean, N=3. All error bars represent SD. The two tailed students t-test was
522 used to determine P-values: *** P < 0.001. B) Calu3 cell protein lysates were probed 48 hours
523 post infection by Western blotting for phosphorylated STAT1 (Y701), STAT1, IFIT2, TRIM25,
524 and Actin.

525 **Figure 4, Conservation of SARS-CoV IFN antagonists.** Viral protein sequences of the
526 indicated viruses were aligned according to the bounds of the SARS-CoV open reading frames

527 for each viral protein. Sequence identities were extracted from the alignments for each viral
528 protein, and a heat map of percent sequence identity was constructed using EvolView
529 (www.evolgenius.info/evolview) with SARS-CoV as the reference sequence. TR = truncated
530 protein.
531

532

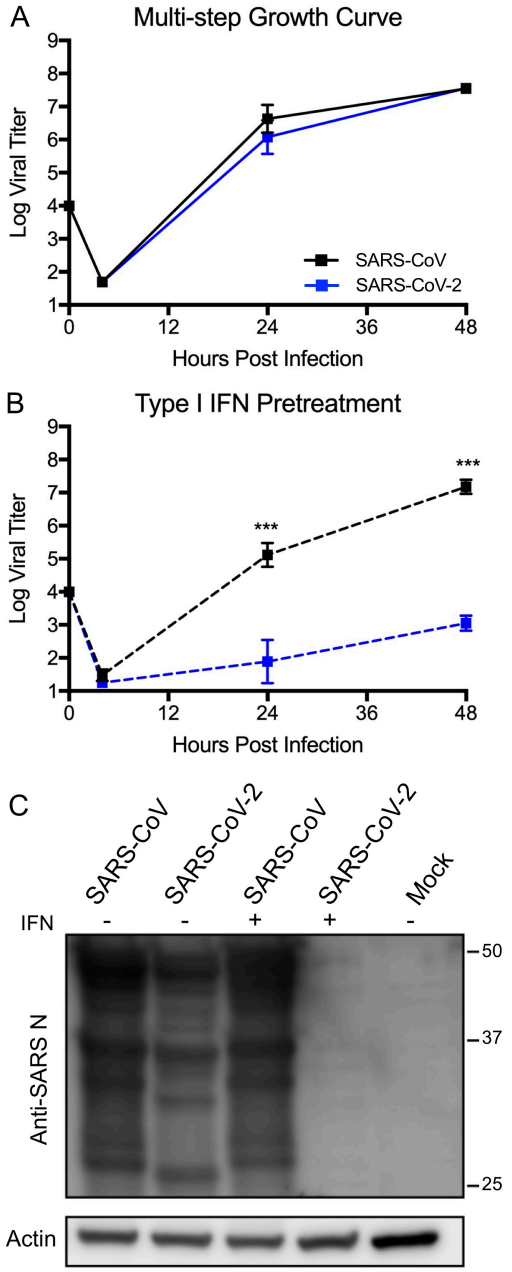

533

534 **Figure 1. SARS-CoV-2 sensitive to type I IFN pretreatment.** A) Vero E6 cells infected with
535 either SARS-CoV WT (black) or SARS-CoV-2 (blue) at an MOI of 0.01. Media harvested at 4,
536 24, and 48 hours post infection. B) Vero E6 cells were treated with 1000 units recombinant type
537 I IFN or mock for 18 hours prior to infection. Cells were subsequently infected at with either
538 SARS-CoV WT (black) or SARS-CoV-2 (blue) at an MOI of 0.01 as described above. Each
539 point on the line graph represents the group mean, N=6 for 24 and 48HPI, N=3 for 3HPI. All
540 error bars represent SD. The two tailed students t-test was used to determine P-values: *** <
541 0.001. C) Cell protein lysates from IFN treated and untreated cells were probed 48 hours post
542 infection by using Western blotting with rabbit polyclonal anti-SARS N antibody or actin.

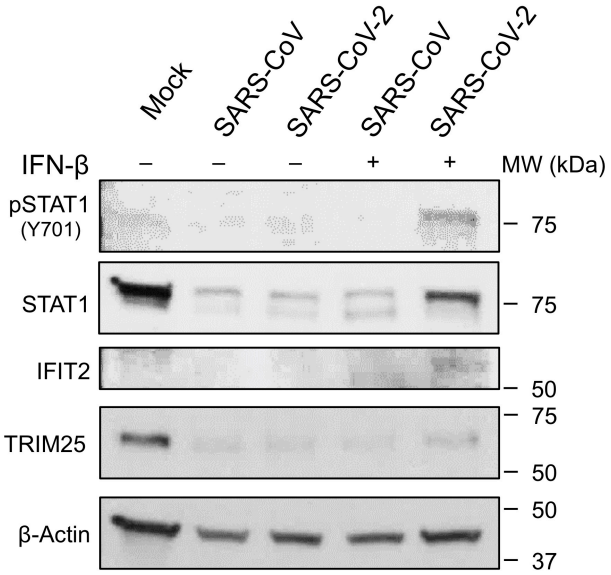

Figure 2. SARS-CoV-2 infection induces STAT1 phosphorylation and ISG production. Vero cell protein lysates from IFN-I treated and untreated cells were probed 48 hours post infection by Western blotting for phosphorylated STAT1 (Y701), STAT1, IFIT2, TRIM25, and Actin.

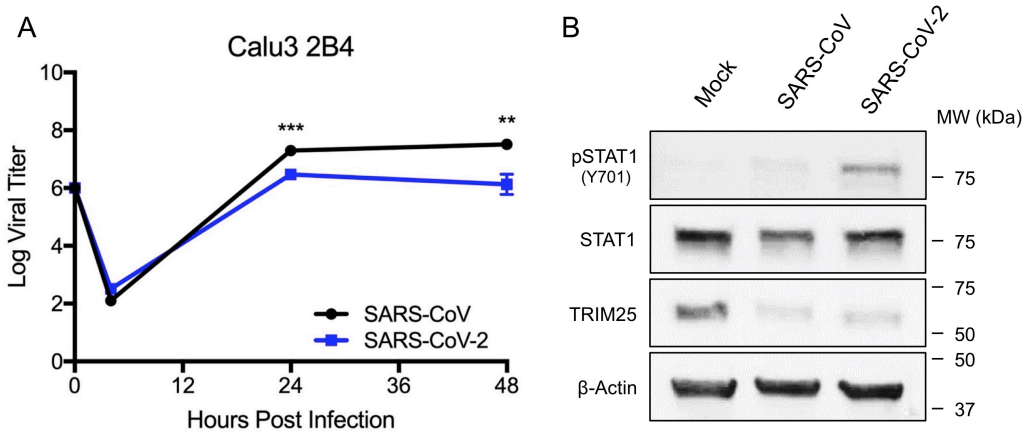

549

550 **Figure 3. SARS-CoV-2 induces STAT1 phosphorylation in IFN competent cells**. A) Calu
551 2B4 cells were infected with either SARS-CoV WT (black) or SARS-CoV-2 (blue) at an MOI of
552 1. Media harvested at 4, 24, and 48 hours post infection. Each point on the line graph
553 represents the group mean, N=3. All error bars represent SD. The two tailed students t-test was
554 used to determine P-values: *** < 0.001 ** < 0.01. B) Calu3 cell protein lysates were probed 48
555 hours post infection by Western blotting for phosphorylated STAT1 (Y701), STAT1, IFIT2,
556 TRIM25, and Actin.

557

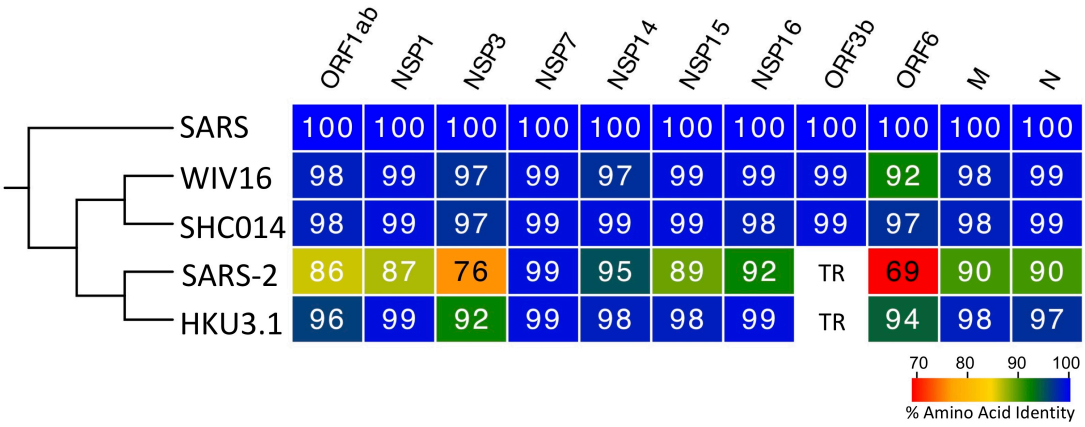

Figure 4, Conservation of SARS-CoV IFN antagonists. Viral protein sequences of the indicated viruses were aligned according to the bounds of the SARS-CoV open reading frames for each viral protein. Sequence identities were extracted from the alignments for each viral protein, and a heat map of percent sequence identity was constructed using EvolView (www.evolgenius.info/evolview) with SARS-CoV as the reference sequence. TR = truncated protein.